Performance parametric analysis of retrofitted Gas turbine cycle using STIG and Evaporative cooling techniques

R.S. Mishra, Shyam Agarwal

Department of Mechanical & Production Engineering, Delhi Technological University Delhi, India

Abstract

The present paper represents the parametric analysis of retrofitted gas turbine cycle on the basis of energy and exergy principles of thermodynamics. The retrofitting techniques i.e. inlet air evaporative cooling (EVC) and steam injection to gas turbine (STIG) have been considered incorporation to the basis gas turbine cycle to investigate the performance of cycle. An Engineering Equation Solver (EES) software program has been developed to explore the effect of ambient temperature and relative humidity of air on various performance parameters i.e. power output, heat rate, thermal efficiency, generation efficiency, first law efficiency, exergetic efficiency and exergy destruction rate. It has been observed that the power output, thermal efficiency, generation efficiency, first law efficiency and exergetic efficiency get enhanced; however, heat rate declines with increase in ambient temperature. The association of combined EVC and STIG technologies to the basic gas registers 45% increment in power output, 4.5% increment in thermal efficiency and 26% enhancement in exergetic efficiency during summer days at 50^0C ambient temperature and 80% relative humidity of ambient air. The combustion chamber is the most sensitive system component in exergy destruction. © 2018 ijrei.com. All rights reserved
Keywords: Gas turbine, Retrofitting, EVC, STIG, Exergy

_____

1. Introduction

The thermodynamic processes of a simple cycle gas turbine can be approximately modeled as a Brayton cycle, in which the back work ratio is usually very high, and the exhaust temperature is often 500 ^{0}C. A high exhaust temperature implies that there is plenty of useful energy has waste to the environment. The recovery of this otherwise waste energy can be used to improve either the power generation capacity or efficiency. Simple gas turbine power generation systems are widely used in Indian industries due to quick startup and shutdown capabilities. These units are mostly used to fulfill the peak load demand but unfortunately suffer from very low overall efficiency and reduction in power output during the summer season, when electricity demand is the highest. To investigate the anticipated power shortage, retrofitting projects have been seriously gaining momentum to covert these existing simple gas turbine systems into relatively advanced cycle units resulting in both improved efficiency and power output.

Various research and development work is going on around the world to reduce the compressor work and simultaneously reduce the heat supplied. The compressor work can be reduced by cooling the inlet air to the compressor. It can be achieved by an efficient and economical spray cooling technique. In which, the ambient air has been cooled by adding spray of water at wet bulb temperature up to its saturation limit in an isolated chamber (spray chamber). The adiabatic mixing of air and water exchange heat and the sensible heat of air has been transferred to the water and the water has become evaporated. In this manner, the addition of water vapour has been taken places to the air and the temperature of the resulting air has been reduced and mass flow rate gets improved by means of fog cooling unit or (EVC) evaporative cooling system. The performance of gas turbines can be enhanced by doing minor modifications in gas turbines without major destruction to its original integrity. One of the most interesting aspect of gas turbine is that waste heat of flue gases can be used in generating steam at high pressure. Higher pressure steam can be used for injection in combustion chamber as STIG (steam injected gas turbine) at different injection ratio from 0 to 0.2. These attractive features can improve the power generation capacity and efficiency of the power generation system to a considerable extent. Again, steam injection can reduce NO_x

_____

and SO$_2$ emissions. These enhancements are nowadays in application in some parts of the world and expected to widen throughout the world because gas turbine is thermo economically advantageous. Performance improvement through retrofitting is the main motivation of this work. Bhargava & Homji [1] have studied parametric analysis of existing gas turbines with inlet evaporative and overspray fogging. This study shows the effects of inlet fogging on a large number of commercially available gas turbines. Chaker et al. [2] have developed the formulation for fog droplet sizing analysis and discussed various nozzle types, measurement and testing. This study describes the different available measurement techniques, design aspects of nozzles, with experimental and provides recommendations for a standardized nozzle testing method for gas turbine inlet air fogging. Sinha & Bansode [3] have studied the effect of fog cooling system for inlet air cooling. They concluded that performance parameters indicative of inlet fogging effects have a definite correlation with the climate condition (humidity and temperature) and showed improvement in turbine power and heat rate. Moran et al. [4] has developed design and economic methodology for the gas turbine cogeneration system. Wang & Chiou [5] suggested that application of IAC and STIG technique can boost the output and generation efficiency. They concluded that implementing both STIG and IAC features cause more than a 70% boost in power and 20.4 % improvement in heat rate. Kumar et al. [6] have been developed design methodology for parametric study and thermodynamic performance evaluation of a gas turbine cogeneration system (CGTS). Pelster et al. [7] studied the combined cycle with advanced options viz. compressor air inter-cooling, water injection and reheating. They studied environmental and economic analysis simultaneously. They have optimized the system for economic and other better operations. Korakianitis et al. [8] investigated parametric performance of combined-cogeneration power plants with various power and efficiency enhancements. The performance of combined-cogeneration power plants is dominated by the gas turbine performance. The performance of these plants is optimized by A. maximizing turbine rotor inlet temperature in the gas turbine. B. Optimizing the gas turbine pressure ratio for gas-turbine performance. C. Optimizing steam turbine boiler pressure and D. Maximizing steam injection in the gas turbine. Hawaj & Mutairi [9] studied a cogeneration system comprising a combined cycle power plant (CCPP) with an absorption chiller used for space cooling. They have also studied the relative advantage of using CCPP with absorption cooling over thermally equivalent mechanical vapor compression (MVC).They found that a cogeneration CCPP with absorption cooling yields significantly less power penalty than a CCPP with a MVC cooling. Facchini [10] has performed the detailed study of reheat gas turbine/combined cycle and close loop steam gas cooled gas turbine. The detailed exergy balance is used in this study to compare the performance of plant sections and to understand the margin for potential improvement. Nishida et al. [11] have analyzed the

performance characteristics of two configurations of regenerative steam-injection gas turbine (RSTIG) systems. They concluded that the thermal efficiencies of the RSTIG systems are higher than those of regenerative, water injected and STIG systems. Many researchers [12-21] have investigated the performance of simple and combined gas turbine cycle. Retrofitted techniques have also explored and it is observed that the retrofitted technologies like inlet air evaporative cooling (EVC) and steam injection to gas turbine improves the performance of the cycle [21].

From the above gathered literature review from different established data sources like Research Gate, Science Direct and Google Scholar etc. It has been concluded that opportunities are available to analyze different retrofitted techniques for gas turbine cycles viz. spray cooling technique, combined evaporative cooling and STIG etc. In this communication, a simple cycle gas turbine unit is considered as base unit and this unit has been retrofitted with fog cooling or EVC (evaporative cooling), STIG (steam injected gas turbine) and combined cycle (fog cooling and STIG both). The performance improvement has been thermodynamically analysed and discussed for above mentioned retrofitted techniques followed by performance studies.

2. Thermodynamic model for parametric analysis

2.1 Description of system

Fig.1 shows the schematic diagram of simple gas turbine integrated to evaporative cooling system (fog cooling system) and STIG system. It consists of an evaporative cooling system (fog cooling system), a compressor, a combustion chamber unit, a simple gas industrial turbine and a HRSG unit. HRSG unit consists of an economizer, an evaporator and a super-heater. Evaporative cooling system consists of nozzles and an isolated chamber (duct) in which adiabatic heat transfer takes place. Pressurized liquid water is sprayed into the duct through nozzles at corresponding wet-bulb temperature. Fog cooling is an evaporative cooling method of cooling the intake air by demineralised water. Water is converted into fog droplets by means of special atomizing nozzles operating at approximately 138bar. The evaporation of small size (5-20 microns) droplets in the intake duct cools the air and consequently increases the mass flow rate. This technique allows close to 100% evaporative effectiveness in terms of attaining saturation conditions and wet-bulb temperature at the gas turbine inlet. The evaporative cooling process works essentially with conversion of sensible heat in latent heat. The surrounding ambient air is cooled by evaporation of water from the wet surface of the panel to the air. The addition of water vapour to the air increases its latent heat and relative humidity. If the process is adiabatic, this increases the latent heat compensated by a reduction of the sensible heat and consequent reduction of the dry bulb temperature of air as shown in Fig. 1.
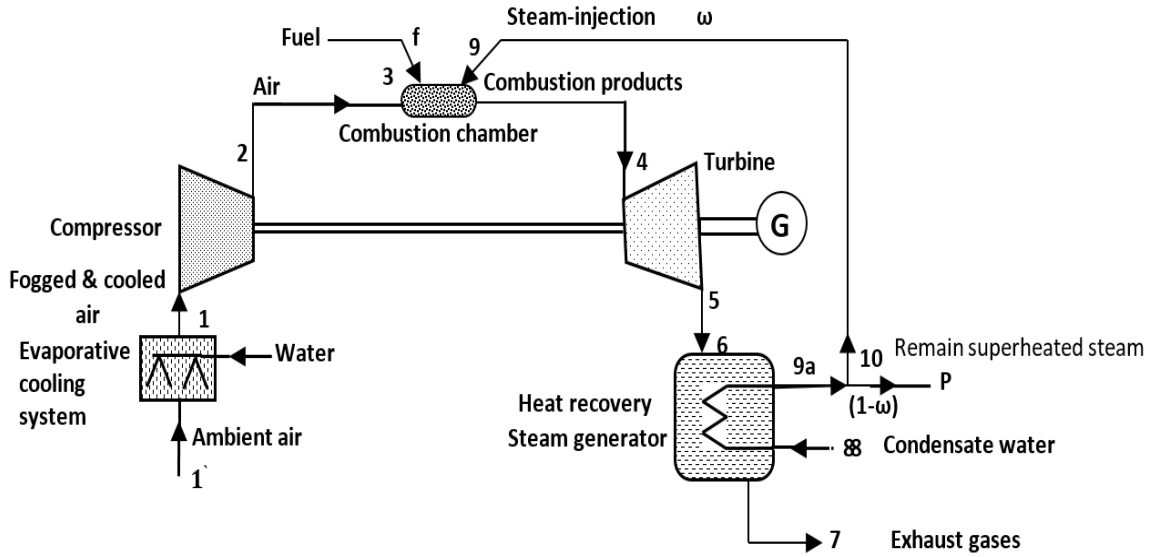
Figure 1: Schematic diagram of Simple gas turbine cycle retrofitted to EVC and STIG
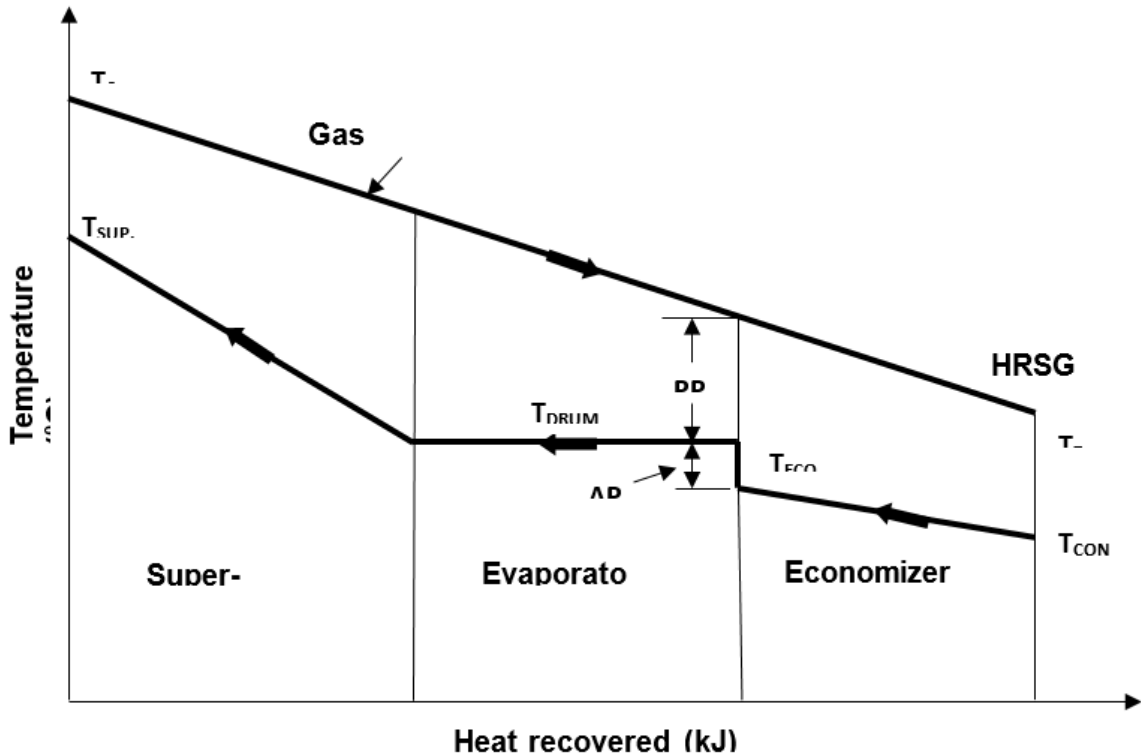
Figure 2: Temperature- heat energy diagram of HRSG

The amount of fog is to be monitored base on dry and wet bulb ambient conditions to achieve the required cooling. A typical fog cooling system consists of a high pressure pump skid connected for feeding to an array of manifolds located at a suitable place across the compressor inlet duct. The manifolds have a requisite number of fog nozzles[6] which inject very fine droplets of water into the inlet air. The discharge through each nozzle is around 3ml/s and produces 3 billion droplets per second. The fine fog evaporates very fast, thus dropping inlet air temperature. The simple cycle gas turbine system integrated to both IAC and STIG feature has been shown in Fig. 1. A heat recovery steam generator (HRSG) has been installed at the downstream exit of the turbine (state point 5) in order to recover the heat from the exhaust gases as shown in Fig.1 and 2. The fraction of superheated steam generated from the HRSG is used for STIG (state point 9) and the remaining steam is used

for process application. HRSG consists of an economizer, evaporator and super-heater. The waste heat received from the exhaust of turbine at the inlet of HRSG at state point 6 converts the condensate water passing through economizer, evaporator and superheat into superheated steam at state 9a as shown in Fig.2. A fraction (ω) of superheated steam is fed to the combustion chamber at state9. The remain superheated steam (1-ω) is available to use in other process applications.

2.2 Mathematical modeling

The current analysis presents the parametric investigations of simple gas turbine cycle which has been retrofitted to evaporative cooling (EVC) and steam injection gas turbine (STIG). The retrofitted techniques improve the performance of the cycle. A computer code has been developed in Engineering Equation Solver (EES) [16] software for the computation of performance parameters. Steady state governing equations based on first and second law of thermodynamics have been formulated for control volume systems. Mass and energy conservation principles have been considered and the following assumptions have been assumed to develop complex thermodynamic model. [4, 20]

- The temperature of combustion chamber is assumed to be constant.
- 100% relative humidity to the ambient air in the evaporative cooling system.
- The ambient air is at dry bulb temperature and having 60% of R.H. (except where the variation has been done).
- The composition of dry and ambient air assumed in terms of molar fraction of 1 mole of air is: ($N_2 = 0.78981$, $O_2 = 0.20989$, $CO_2 = 0.00031$ and $H_2O = 0$) & ($N_2=0.7748$, $O_2=0.2059$, $CO_2=0.00030$ and $H_2O=0.0190$).
- The fuel (natural gas) is taken as methane modeled as an ideal gas. The fuel is provided to the combustion chamber at the required pressure.
- The combustion in the combustion chamber is complete and N_2 is assumed as inert gas.
- The pressure of water injected from the nozzle into the evaporative cooling chamber has been assumed 138 bar.

A set of governing equations for a particular component (k) is expressed as:

Mass rate balance
$$\sum_i \dot{m}_{i,k} = \sum_e \dot{m}_{e,k} \tag{1}$$
Energy balance
$$\dot{Q}_{cv,k} - \dot{W}_{cv,k} = \sum_e \dot{m}_{e,k} h_{e,k} + \sum_i \dot{m}_{i,k} h_{i,k} \tag{2}$$
Exergy balance
$$\dot{E}_{D,k} = \sum \dot{E}_{q,k} - \dot{W}_{cv,k} + \sum_i \dot{E}_{i,k} - \sum_e \dot{E}_{e,k} \tag{3}$$

2.3 Evaporative cooling system

$$\dot{m}_w(h_{v1} - h_{w1}) = \dot{m}_a(h_{a1`} - h_{a1}) + \omega_{1`}\dot{m}_a(h_{v1`} - h_{v1}) \tag{4}$$

where $\dot{m}_w$ is the mass flow rate of cooling water and $h_{w1`}$ is its enthalpy, $\dot{m}_a$ is the mass flow rate of dry air ($h_{a1`} - h_{a1}$) is the enthalpy change of dry air, $\omega_{1`}$ is the humidity ratio (specific humidity ) of inlet-air in kg of water per kg of dry air, and ($h_{v1`} - h_{v1}$) is the enthalpy change of water vapour after cooling.

The humidity ratio ($\omega_{1`}$) can be specified directly or calculated from:

$$\omega_{1`} = \frac{0.622 P_{v1`}}{P_{1`} - P_{v1`}} \tag{5}$$

Where $P_{v1`}$the partial pressure of water is vapour and $P_{1`}$ is the total atmospheric pressure. From conservation of mass, the amount of water sprayed is equal to the mass of water vapour at point 1minus the water vapour originally in the air at point1'.

$$\dot{m}_w = (\omega_1 - \omega_{1`})\dot{m}_a \tag{6}$$

where ω_1 is the humidity ratio of air after cooling, which can also be specified directly or found from the Eq.(3.56) if $P_{v1`}$ is replaced by $P_{v1}$. The partial pressure of water vapour at point $1`$ and 1 can be found from the respective relative humidity (ϕ), which is given by equation (7)

$$P_{v1} = \phi_1 P_{sat1} \tag{7}$$

Where $P_{sat1`}$ and $P_{sat1}$ are the saturation pressures of water at the corresponding temperatures ($T_{1`}$ or T_1). Neglecting pressure losses in the process and P_1 is equal to $P_{1`}$.

2.4 Heat Recovery Steam Generator

The superheated steam generated $\dot{m}_{S,SUP}$for each kg/s of exhaust gases can be determined by applying the mass and energy conservation principles across superheater and economizer as:

$$\dot{m}_{S,SUP}(h_{S,SUP} - h_{COND}) = \dot{m}_P(h_6 - h_7) \tag{8}$$

Where $h_{S,SUP}$the enthalpy of superheated steam is generated in HRSG, h_{COND} is enthalpy of condensate water at inlet to HRSG, $\dot{m}_P$ is mass flow rate of flue gases, h_6 and h_7 are enthalpy of flue gases at inlet and exit of HRSG respectively.

2.5 Exergy destruction in HRSG

$$\dot{E}_{D,HRSG} = \dot{E}_6 - \dot{E}_7 + \dot{E}_8 - \dot{E}_9 \tag{9}$$

2.6 Compressor

In a compressor, a gas is caused to flow in the direction of increasing pressure and/or elevation by means of a mechanical or electrical power input which is given by:

$$\dot{W}_C = \dot{m}_a(h_2 - h_1) \tag{10}$$

Where h_2 and h_1 are specific enthalpies at state point 2 and 1 respectively.

$$\eta_C = \frac{(h_{2s} - h_1)}{(h_2 - h_1)} \tag{11}$$

Where h_{2s} is the isentropic specific enthalpy at state point 2.

2.7 Exergy destruction in compressor

$$\dot{E}_{D,C} = W_C + \dot{E}_1 - \dot{E}_2 \tag{12}$$

Where $\dot{E}_1$ and $\dot{E}_2$ are exergy at state point 1 and 2.

2.8 Combustion chamber

$$\frac{n_f}{n_a} = \lambda \tag{13}$$

$$\frac{n_P}{n_a} = 1 + \lambda \tag{14}$$

Where the subscripts f, p and a denote fuel, combustion products & air respectively and λ is the fuel-air ratio.
For complete combustion of natural gas (methane) with steam injection (Fig. 1) in the combustion chamber, chemical equation takes the following form:

$$\bar{\lambda} CH_4 + [X_{1,N_2}N_2 + X_{1,O_2}O_2 + X_{1,CO_2}CO_2 + X_{1,H_2O}H_2O] + \omega \to [1 + \bar{\lambda} + \omega][X_{2,N_2}N_2 + X_{2,O_2}O_2 + X_{2,CO_2}CO_2 + X_{2,H_2O}H_2O] \tag{15}$$
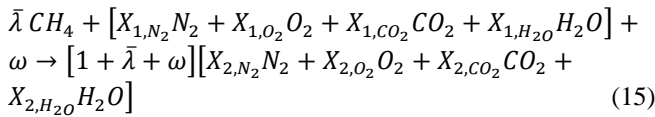
Where ω is the steam injection ratio defined as the ratio of mass of steam injected to the mass of inlet air.

$$\omega = \frac{\dot{m}_s}{\dot{m}_a} \tag{16}$$

$$\omega = \left(\frac{\dot{m}_s}{\dot{m}_f}\right) \times \left(\frac{\dot{m}_f}{\dot{m}_a}\right) \tag{17}$$

$$\omega = \omega`(1 + \lambda) \tag{18}$$

$$\omega` = \frac{\dot{m}_s}{\dot{m}_g} \tag{19}$$

$$\omega`` = \frac{\omega_s}{\omega_f} \tag{20}$$

Where ω'is the ratio of mass of steam injected to the mass of combustion gases formed. $\dot{m}_s$ and $\dot{m}_f$ are the mass rate of steam injected and mass rate of combustion gases formed respectively. λ is the fuel-air ratio.

2.9 Exergy destruction in combustion chamber

$$\dot{E}_{D,CC} = \dot{E}_3 + \dot{E}_f - \dot{E}_4 \tag{21}$$

The isentropic efficiency of turbine is given by eq. (22)

$$\eta_T = \frac{h_4 - h_5}{h_4 - h_{5s}} \tag{22}$$

Where η_T is isentropic efficiency of turbine, h_4 and h_5 are enthalpies of flue gas at state 4 and 5. h_{5s} is the isentropic enthalpy at turbine exit.

2.10 Exergy destruction in turbine

$$\dot{E}_{D,T} = \dot{E}_6 + \dot{E}_4 - \dot{E}_5 \tag{23}$$

2.11 Exergy destruction of stack-losses

$$\dot{E}_{D,Stack-losses} = \dot{E}_7 \tag{24}$$

Thermal Efficiency (η_{Th}): Thermal efficiency of a thermal system is defined as the ratio of net work output $(\dot{W}_{net})$ to the total heat input of the fuel$(\dot{Q}_f)$.

$$\eta_{Th} = \frac{\dot{W}_{net}}{\dot{Q}_f} \tag{25}$$

2.12 First–Law Efficiency (η_I)

The ratio of all the useful energy extracted from the system (electricity and process heat) to the energy of fuel input is known as first-law efficiency. First-law efficiency is also known as fuel utilization efficiency or utilization factor or energetic efficiency.

$$\eta_I = \frac{\dot{W}_{El} + \dot{Q}_{Pro}}{\dot{Q}_f} \tag{26}$$

Where $\dot{W}_{El}$ and $\dot{Q}_{Pro}$ are electric work done and process heat rate respectively.

2.12.1 Heat-Rate (HR)

Heat rate is defined as the ratio of heat rate produced by the fuel to the electrical power out of the thermal system.

$$HR = \frac{\dot{Q}_f}{W_{el}} \tag{27}$$

2.13 Second–Law Efficiency (η_{II})

Since exergy is more valuable than energy according to the second law of thermodynamics, it is useful to consider both output and input in terms of exergy. The amount of exergy supplied in the product to the amount of exergy associated with the fuel is a more accurate measure of thermodynamic performance of a system, which is called second-law efficiency. It is also called exergetic efficiency (effectiveness or rational efficiency).

$$\eta_{II} = \frac{\dot{W}_{El} + \dot{E}_{Pro}}{\dot{E}_f} \qquad (28)$$

Where $\dot{E}_{Pro}$ the exergy is content of process heat and $\dot{E}_f$ is the exergy content of fuel int.

2.14 Effectiveness (Exergetic efficiency) of component (ε)

Exergetic efficiency of component is defined as the ratio of exergy rate recovered from the component $(\dot{E}_R)$ to the exergy rate supplied to the component $(\dot{E}_S)$. Exergetic efficiency gives true measure of useful energy which cannot be obtained from energy criteria.

$$\varepsilon = \frac{\dot{E}_R}{\dot{E}_S} = \frac{\dot{E}_R}{\dot{E}_R + \dot{E}_D} = 1 - \frac{\dot{E}_D}{\dot{E}_R + \dot{E}_D} \qquad (29)$$

2.15 Exergy-Destruction Rate $(\dot{E}_{D,R})$

The component exergy destruction rate can be compared to the total exergy destruction rate within the system.

$$\dot{E}_{D,R} = \frac{\dot{E}_D}{\dot{E}_{D,Total}} \qquad (30)$$

2.16 Exergy-Destruction Rate(MW)per MW of Power Output

It is defined as the ratio of exergy destruction rate of component $(\dot{E}_{D,k})$ to the net power output $(\dot{W}_{net})$ of the system cycle.

$$\dot{E}_{D,R/MWP} = \frac{\dot{E}_{D,k}}{\dot{W}_{net}} \qquad (31)$$

3. Results and discussions

The present work analyzed a retrofitted simple gas turbine cycle incorporated to evaporative inlet air cooling (EVC) and steam injection to gas turbine (STIG) techniques energetically and energetically. A computer program has been developed in Engineering Equation Solver (EES) [16] software to compute the performance parameters (Power output, Thermal efficiency, First law efficiency, exergetic efficiency, exergy destruction rate). The effect of ambient temperature has been observed on various performance parameters.

Table 1: Input parameters of retrofitted simple gas turbine cycle Moran et al.[4]and Agarwal et al.[20]

S.N	Input parameters	Numerical values
1.	Ambient air temperature, pressure and relative humidity at state point 1`	25^0C, 1.013bar & 60%
2.	Spray water temperature and pressure at state point1`	25^0C, 138bar
3.	Inlet air temperature, pressure and relative humidity (T_1, P_1 & ϕ_1) to compressor at state point 1	25^0C, 1.013bar & 100%
4.	Pressure ratio of compressor (r_P)	10:1
5.	Isentropic efficiency of compressor (η_C)	0.86
6.	Isentropic efficiency of turbine (η_T)	0.86
7.	Mass flow rate of air ($\dot{m}_a$)	81.4 kg/s
8.	Lower heating value of fuel	802361 kJ/kmol
9.	Turbine inlet temperature (TIT) (T_4)	1247^0C
10.	Injection temperature and pressure of fuel (T_f, P_f)	25^0C, 12bar
11.	Exhaust temperature and pressure of combustion products after HRSG (T_7, P_7)	130^0C, 1.013 bar
12.	Temperature and pressure of condensate water at inlet of HRSG (T_8, P_8)	25^0C, 20 bar
13.	Steam generation pressure (P_{9a})	20 bar
14.	Pressure drop in combustion chamber and HRSG on gas side	5%
15.	Amount of steam injected (ω), (% of the mass flow rate of the air)	10%
16.	Temperature of superheated steam STIG (T_9)	480^0C
17.	Approach and pinch point	2^0C, 20^0C

3.1 Model Validation

The results of current analysis have been compared to Moran et al. [4] and Agarwal et al. [20] as shown in Table2. The variation in the results is within ±1%. The variation is due to the consideration of pressure drop in combustion chamber and HRSG.

3.2 Parametric Analysis

3.2.1 Effect of ambient temperature on percentage power

output difference with respect to simple cycle.

Fig. 3 shows that the variation of percentage power output difference with ambient temperature for wide range of relative humidity for evaporative cooling cycle (EVC) as compared to simple cycle.
As the temperature of ambient air increases, the power output of simple cycle decreases due to decrease in density of air for a specified relative humidity. For a constant volume machine, decrease in density of air reduces the mass flow rate of air
Table 2: Comparison of operational parameters ($\dot{m}$, P, T)(a:Simple

cycle, b:Simple+EVC, c:Simple+STIG, d:simple+EVC+STIG)[4, 20]

State points	Mass flow rate ($\dot{m}$) kg/s			
	a	b	c	d
1`	---	81.4, 1.14		81.4, 1.14
1	81.4	82.54	81.4	82.54
2	81.4	82.54	81.4	82.54
4	83.36	84.56	91.79	92.98
5	83.36	84.56	91.79	92.98
7			91.79	92.98
8			21.23	21.51
9			8.14	8.14
P			13.09	13.37
f	1.96	2.01	2.247	2.297
Temperature (T) K				
1`	---	298.15, 292.6		298.15, 292.6
1	298.15	292.62	298.15	292.62
2	604.95	594.75	604.95	594.75
4	1520	1520	1520	1520
5	985.6	985.95	1006.15	1006.15
7			403.15	403.15
8			298.15	298.15
9			753.15	753.15
P			753.15	753.15
f	298.15	298.15	298.15	298.15
Pressure (P) bar				
1`	---	1.013, 138		1.013,138
1	1.013	1.013	1.013	1.013
2	10.13	10.13	10.13	10.13
4	9.62	9.62	9.624	9.624
5	1.013	1.013	1.066	1.066
7			1.013	1.013
8			20	20
9			20	20
P			20	20
f	12	12	12	12

It is interesting to observe that the difference in power output for with or without evaporative cooling at given R.H. increases with increasing temperature due to increase in intake mass flow rate of air (mass flow rate of ambient air + mass flow rate of fog water) and at lower temperature. The percentage difference in power output is lower for high R.H. line while higher for a low R.H. line because the higher amount of water vapour added to the air at low R.H. during evaporative cooling

(fog cooling) to get saturated air which increases the overall mass flow rate of air. At high temperature the saturation capacity of air increases (i.e. at high temperature and R.H., amount of water vapour required to obtain 100% saturation is more than at low temperature) due to which there is significant increase in mass flow rate and hence power output increases rapidly and the effect can be observed in the Fig. 3 such that the 80% R.H. line coincide with 60% R.H. line at 50°C.
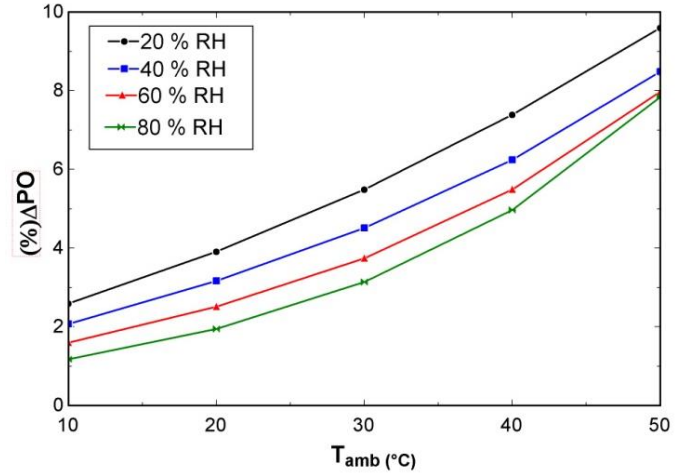
Figure 3: Effect of ambient temperature on % difference in power output (Simple cycle+EVC)

Fig. 4 shows a significant increase in power output for STIG (steam injected gas turbine) due to increase in mass flow rate of intake air to the turbine (mass flow rate of air from compressor + mass flow rate of STIG). It reflects that the variation in percentage power output difference with temperature and relative humidity for STIG cycle with respect to simple cycle.
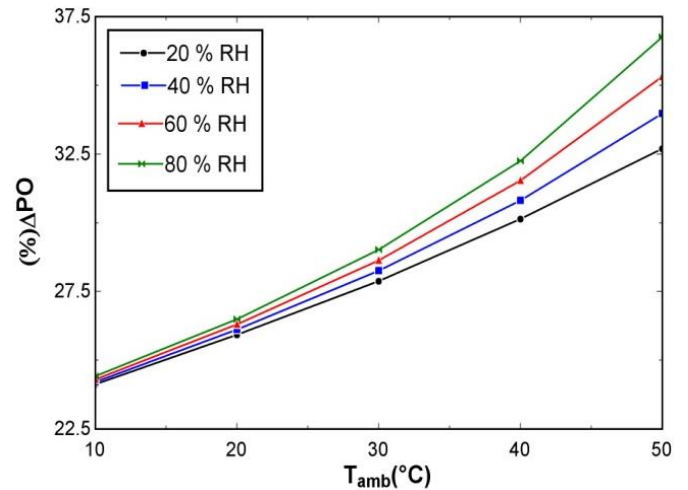
Figure 4: Effect of ambient temperature on % difference in power output (Simple cycle+STIG)

At constant ambient temperature the percentage power output

difference is higher for high R.H. value and lower for low R.H. value because for high R.H. value, the intake mass flow rate of air to compressor (mass flow rate of dry air + mass flow rate of water vapour contents) increases. As the temperature of ambient air increases the density of air decreases, so the intake mass flow rate of air to compressor decreases with the same rate for simple cycle as well as for STIG cycle. Though the ambient temperature increases the power output for both the cycles decreases for a constant R.H. condition yet the percentage power output difference increases. The reason is that at higher temperature the power output of simple cycle falls rapidly while the power output of STIG cycle fall gradually (as the STIG steams has higher latent heat).

Combined effect of evaporating cooing and STIG has been shown in Fig. 5. As the mass flow rate of air increases during evaporating cooling (mass flow rate of air from compressor + mass flow rate of STIG) and for STIG (mass flow rate of air from compressor + mass flow rate of STIG) , the increase in power output is higher than that of EVC and STIG cycle.

R.H. value. As the R.H. lines gets diversed and more steep for high R.H. value, the moisture contents are higher for higher D.B.T. and R.H.

3.2.2 Effect of ambient temperature on percentage heat-rate difference with respect to simple cycle

Fig. 6 shows the variation of percentage heat rate difference with ambient temperature for wide range of relative humidity for evaporative cooling cycle as compared to simple cycle. For a constant R.H. value as the temperature of ambient air increases the mass flow rate of air intake air to compressor decreases due to reducing density results reducing electrical work output and mass of fuel consumed and hence heat rate falls rapidly. It has been observed that the heat rate falls rapidly for low R.H. as compared to higher R.H. for a constant temperature due to high air fuel ratio which increases heat flow rate for high R.H. values and the difference between two heat rates for EVC cycle and simple cycle reduces.

Figure 5: Effect of ambient temperature on % difference in power output (Simple cycle+EVC+STIG)
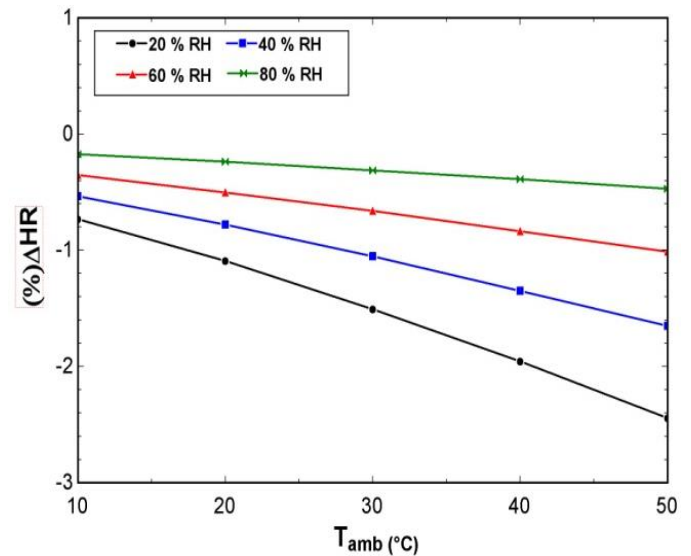
Figure 6: Effect of ambient temperature on % difference in heat rate (Simple cycle+EVC)

Fig.5 shows the variation in percentage power output difference with temperature and R.H. At a constant temperature, the percentage difference in power output is higher for low R.H. value than that of high R.H. value due to high mass flow rate of intake air to compressor (mass flow rate of dry air + mass flow rate of water vapour). At low R.H ambient conditions air reuqires higher amount of water vapour to get saturated. The increase in ambient temperature lowers the mass flow rate of air but the difference in power output is higher due to rapid fall in power out of simple cycle. At high temperature and high R.H. value the the amount of water vapour added to air is higher to get saturated air. Thus the percentage difference in power output jumps suddenly for 50^0C and 80% R.H. It can be observed form the psychometric chart that the humidity ratio is higher for high D.B.T. and high

The gap between high R.H. is less at high temperature and high R.H. because at high temperature and R.H. the larger amount of water vapours are required to get saturated air.

The variation of percentage heat rate difference with ambient temperature for wide range of relative humidity has been shown in Fig. 7. As the ambient temperature increases the density of air decreases and the mass flow rate of combustion products decreases and mass of STIG remains constant so, the total mass of combustion products decreases and heat rate decreases with increasing temperature for a constant R.H. value.
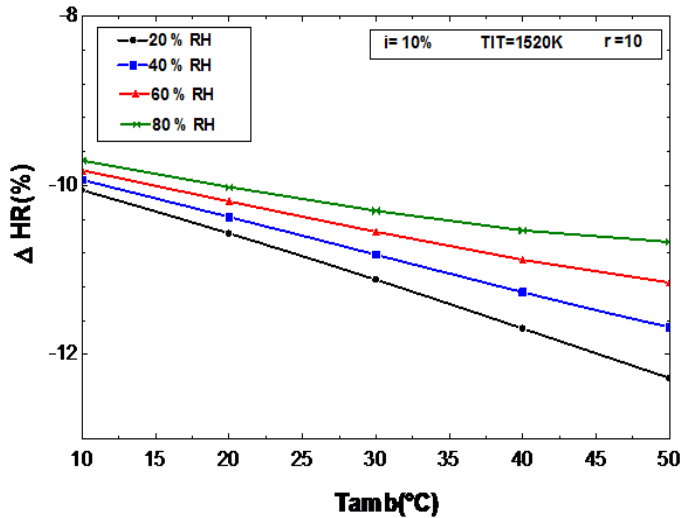
Figure 7: Effect of ambient temperature on % difference in heat rate (Simple cycle+STIG)

On the other hand, the mass flow rate of intake air to compressor decreases rapidly with increasing temperature for a constant R.H. value and hence the difference of heat rate between simple cycle and STIG cycle increases. At a constant temperature, the decrease in heat rate is higher for high R.H. and lower for low R.H. because the mass flow rate of air increases with increasing R.H.

Fig. 8 shows the variation percentage heat rate difference with ambient temperature along wide range of R.H. for combined evaporative and STIG cycle.
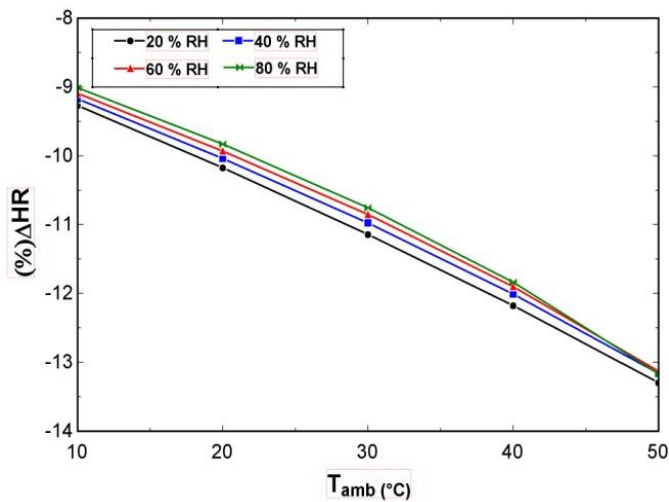
Figure 8: Effect of ambient temperature on % difference in heat rate (Simple cycle+EVC+STIG)

As the temperature of ambient air increases at constant R.H. value the mass flow rate of combustion product (mass of air+mass of fuel+mass of STIG) reduces rapidly as compared to mass of fuel consumed so that the power output decreases and hence the heat rate increases. The heat rate difference between simple cycle and combined cycle decreases with

increase in ambient temperature as the heat-rate increases rapidly for simple cycle. It is an interesting fact that the heat rate falls rapidly for low R.H. as compared to higher R.H. for a constant temperature due to high air fuel ratio (les mass of fuel consumed) which increases heat flow rate for high R.H. values and the difference between two heat rates for combined cycle and simple cycle reduces. At high temperature (50^0C) and R.H. (80%), the heat rate falls rapidly as the amoun of water vapour added to the air increases (as the R.H. lines gets diverged and more steep for high R.H. value at the psychometric chart, the moisture contents are higher for higher D.B.T. and R.H.) and hence high R.H. line coincides with low R.H. lines at high temperature (50^0C) and R.H. (80%).

3.2.3 Effect of ambient temperature on thermal efficiency difference with respect of simple cycle (comparison of retrofitted cycles)

Fig. 9 predicts variation in thermal efficiency (%) difference with temperature along wide range of R.H. for EVC cycle. As the mass flow rate of air decreases with increasing temperature for a constant R.H. value due to rapid decrease in density of air as compared to mass flow rate of fuel consumed and hence the thermal efficiency decreases rapidly for simple cycle. On the other hand, the thermal efficiency of EVC cycle decreases slowly as compared to simple cycle. Hence the difference becomes wider for a particular R.H. with increasing temperature. For constant temperature and low R.H.(20%), the moisture contents added to the air during evaporative cooling are higher to get saturated therefore the difference in thermal efficiency is higher for lower R.H.
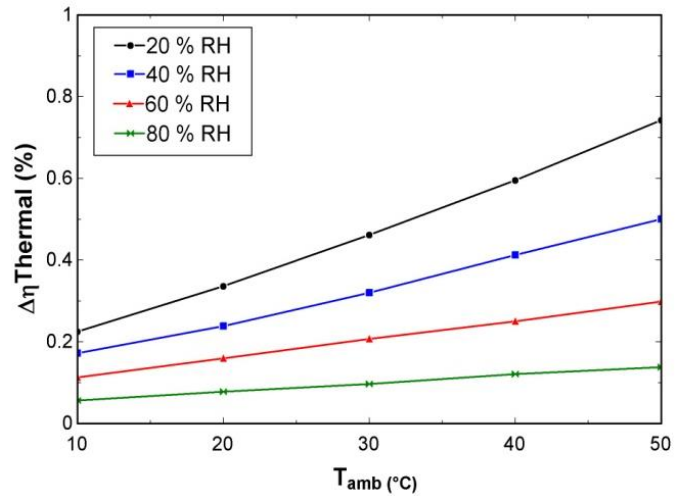
Figure 9: Effect of ambient temperature on % difference in thermal efficiency (Simple cycle+EVC)

The gap among lower R.H. lines is more than that of high R.H. line due to higher moisture contents added to air at high ambient temperature (50^0C) and R.H. (80%) (as the humidity ratio increases rapidly for high D.B.T. and R.H. at

psychometric chart). The variation in thermal efficiency (%) difference with temperature along wide range of R.H. for STIG cycle has been shown in Fig. 10.
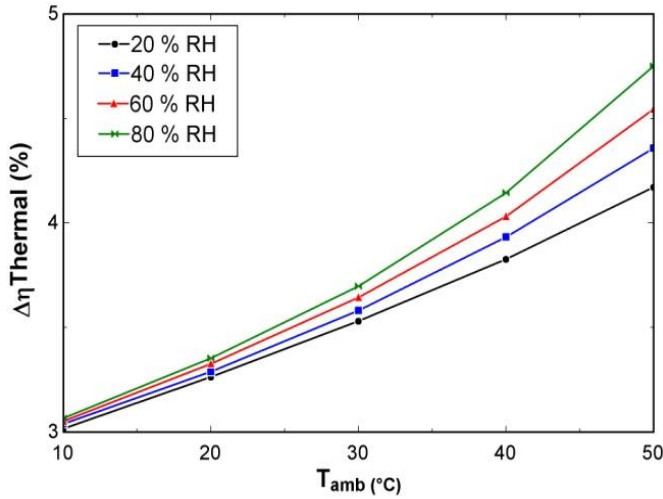
Figure 10: Effect of ambient temperature on % difference in thermal efficiency (Simple cycle+STIG)

As the temperature of air increases for a constant R.H., the density of air decreases, the mass flow rate of air and mass flow rate of fuel consumed decreases as well as the mass of STIG decreases hence mass of combustion products decreases rapidly for simple cycle as compared to STIG cycle by which difference in thermal efficiency (%) increases. The difference in thermal efficiency (%) is higher for high value as compared to low R.H. value at a constant temperature. At high R.H., the mass of water vapour contents are higher which increases mass flow rate of air and ultimately thermal efficiency.

Fig. 11 shows the variation in thermal efficiency (%) with temperature along wide range of R.H. for combined cycle.
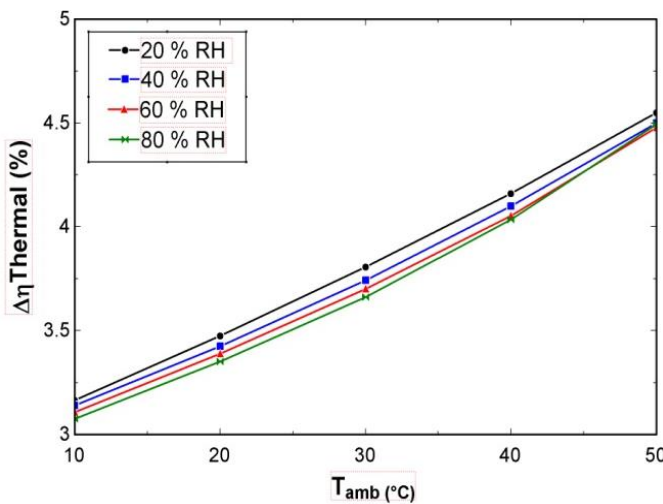
Figure 11: Effect of ambient temperature on % difference in thermal efficiency (Simple cycle+STIG)

As the mass flow rate of combined cycle enhances by two ways (a) using evaporative cooling, the amount of water vapour added (b) the amount of STIG added to the air, and the mass flow rate of fuel consumed also decreases with increasing temperature at constant R.H. value as the air fuel ratio increase. Hence the mass flow rate of combustion products has become higher than that of an individual cycle and difference in thermal efficiency increases. As ambient air at low R.H. value requires high amount of water vapour to get saturated therefore the difference in thermal efficiency (%) is higher for low R.H. value as compared to low R.H. value at constant ambient temperature. At high temperature the gap among high R.H. lines becomes wider due to higher moisture contents added to air at high ambient temperature (50^0C) and R.H. (80%) (as the humidity ratio increases rapidly for high D.B.T. and R.H. at psychometric chart).

3.2.4 Effect of ambient temperature on first-law efficiency (comparison of simple and retrofitted cycles)

Fig. 12 shows the variation of first law efficiency (%) with temperature for various cycles.
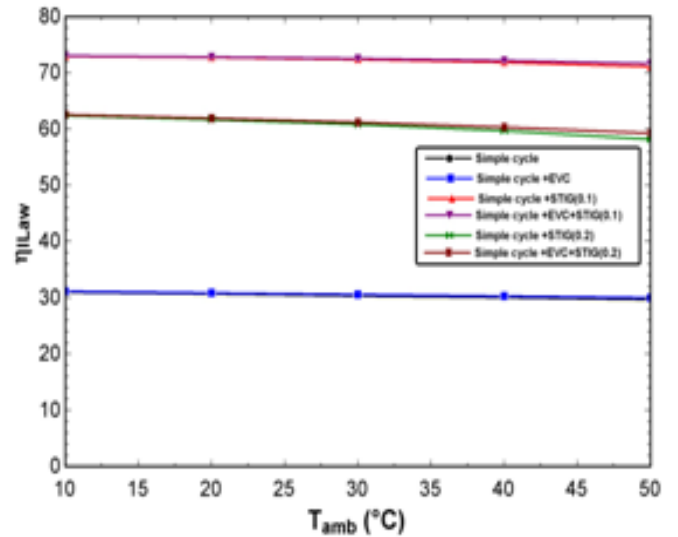
Figure 12: Effect of ambient temperature on first law efficiency for retrofitted cycles

As the temperature of ambient air increases for a constant R.H. value, the mass flow rate of intake air decreases by which power output and process heat available in exhaust gases also decreases. As the air-fuel ratio increases, the mass flow rate of fuel consumed decreases result the first law efficiency remains constant for a specified cycle. As the water vapours contents increases during evaporative cooling, the mass flow rate of intake to compressor increases results power output and process heat increases minutely for EVC cycle. Hence, first law efficiency for EVC cycle coincides with simple cycle. As the amount of STIG added to the air is more significant for

STIG cycle, the mass flow rate of combustion products increases results increase in power output and process heat and the increase in air fuel ratio reduces the mass flow rate of fuel consumed results higher first law efficiency for STIG cycle as shown in fig. 13. The amount of STIG (0.2) cycle imparts large amount of STIG to the air which increases large amount of mass flow rate of air as compared to STIG (0.1) cycle results higher first law efficiency for STIG (0.2) cycle. Combined cycle for STIG (0.1) coincides with STIG (0.1) cycle and combined cycle (0.2) coincides with STIG (0.2) cycle as the effect of evaporative cooling is no much significant.

3.2.5 Effect of ambient temperature on power output and generation efficiency (comparison of simple and retrofitted cycles)
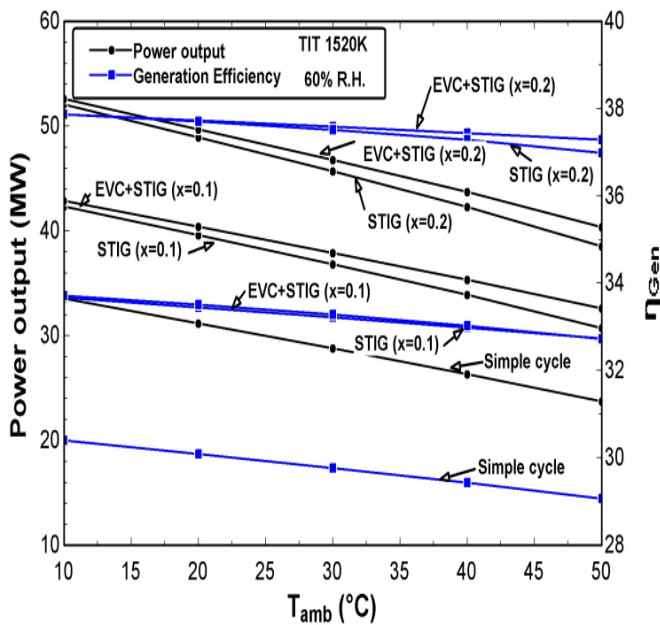
Figure 13: Variation in power output, generation efficiency with ambient temperature for retrofitted cycles

Fig. 13 shows the variation of power output and generation efficiency with ambient temperature at constant R.H. condition (60%) for different cycles. As the ambient temperature increases, the density of air decreases for constant volume machine (compressor and turbine) results mass flow rate of intake air decrease by which mass flow rate of STIG also decreases. Hence the power output decreases for different cycles. The increase in air fuel ratio reduces the mass flow rate of fuel consumed by which generation efficiency reduces gradually for different cycles.

Fig. 14 shows the variation of power output and generation efficiency with relative humidity at constant temperature.
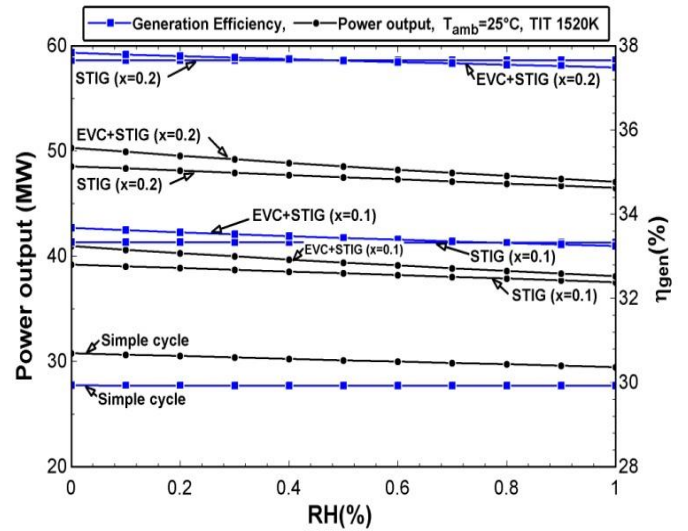
Figure 14: Variation in power output, generation efficiency with relative humidity for retrofitted cycles

. At low temperature, the density of air is higher and the addition of water vapour reduces the average density of air by which power output decreases with increasing R.H. for different cycles while the generation efficiency remains constant due to slight increase in air fuel ratio.

3.2.6 Effect of ambient temperature on second-law efficiency difference with respect to simple cycle (comparison of retrofitted cycles)

Fig. 15 shows the variation in second law efficiency (%) difference with temperature along wide range of R.H. for EVC cycle.
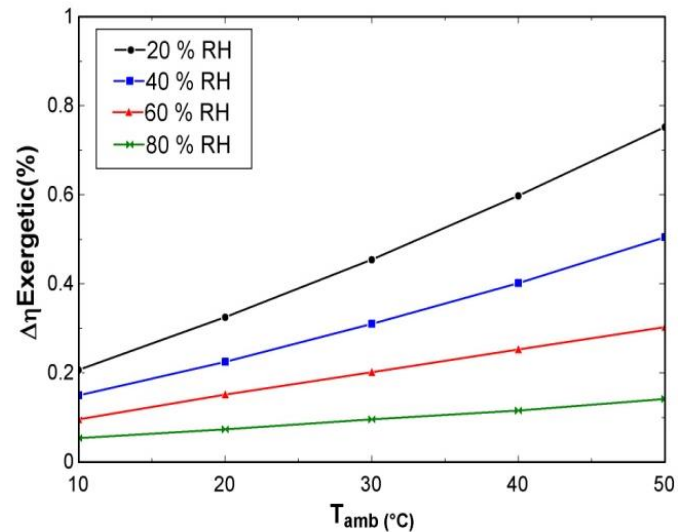
Figure 15: Variation in % difference in exergetic efficiency with ambient temperature (Simple cycle+EVC)

As the temperature of ambient temperature of air increases for a constant R.H. value, the mass flow rate decreases due to decrease density of air by which power output decreases and the exergy of fuel decreases rapidly for simple cycle as compared to EVC cycle. Therefore the difference in exergetic efficiency (%) for simple cycle and EVC cycle increases. For a constant ambient temperature the exertetic efficiency is higher for lower R.H.(20%) condition as compared high R.H.(80%) due to the moisture contents added to the air for low R.H. during evaporative cooling are higher to get saturated air.
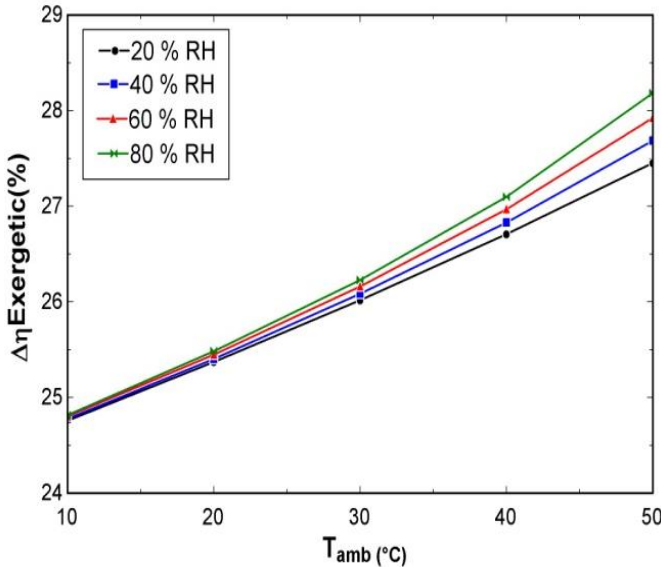
Figure 16: Variation in % difference in exergetic efficiency with ambient temperature (Simple cycle+STIG)

Fig. 16 shows the variation in second law efficiency (%) difference with temperature along wide range of R.H. for STIG cycle. As the temperature of ambient air increases for constant R.H. value, the decreasing mass flow rate reduces power output and mass flow rate of STIG and the mass flow rate of fuel also decreases by which exergy of fuel and exergy of STIG decreases and the exergy of intake ambient air first decreases and then increases hence the second law efficiency increases for STIG cycle and the second law efficiency of simple cycle decreases rapidly results the increase in difference between heat rate for STIG cycle and simple cycle. The second law efficiency is higher for high R.H. as compared to low R.H. for a constant temperature as the the moisture contents are higher for high R.H.

Fig. 17 shows the variation in second law efficiency (%) difference with temperature along with wide range of R.H. for combined cycle.
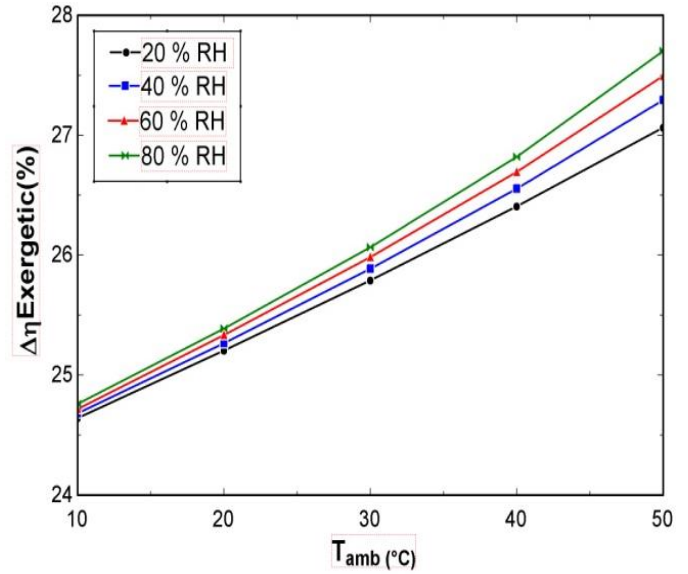
Figure 17: Variation in % difference in exergetic efficiency with ambient temperature (Simple cycle+EVC+STIG)

As the temperature of ambient air increases for a constant R.H., the power output decreases and the mass flow rate of fuel consumed decreases hence the second law efficiency first increases and then decreases for combined cycle while the second law efficiency decreases rapidly for simple cycle and hence the difference in second law efficiency (%) for simple cycle and combined cycle increases. The second law efficiency is higher for high R.H.(80%) condition as compared to low R.H.(20%) for a constant temperature due to decrease in power output is less and the exergy of intake air and fuel reduces sharply.

3.2.7 Comparison of simple and retrofitted cycles for exergy-destruction rate of system components

Fig. 18 shows the exergy destruction rate (MW) for different system components of simple and retrofitted cycles. As the mass flow rate of air increases due to addition of water vapours during evaporative cooling the rate of exergy destruction of compressor increases for EVC cycle and combined cycles. The exergy destruction rate of combustion chamber, gas turbine and HRSG also increases for retrofitted cycles as compared to simple cycle. As the mass flow rate of air also increases due STIG amount, the exergy destruction rate (MW) for combustion chamber, gas turbine and HRSG increases while the compressor remains unaffected.
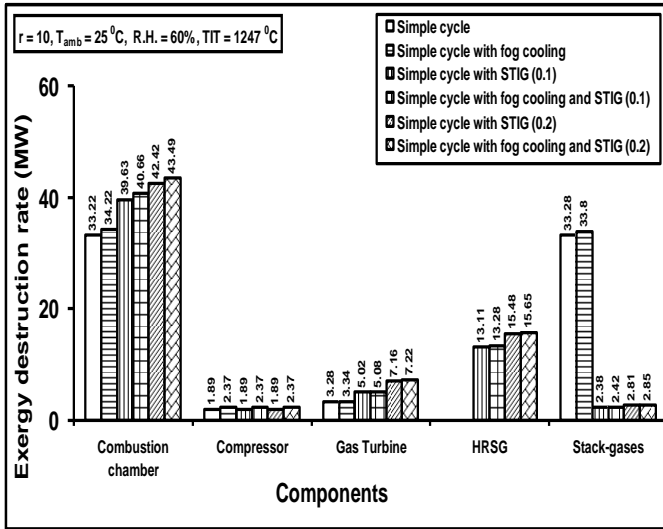
Figure 18: Exergy destruction rate (MW) of system components for simple and retrofitted cycles

increases (maximum for combined cycle with STIG (0.2)).
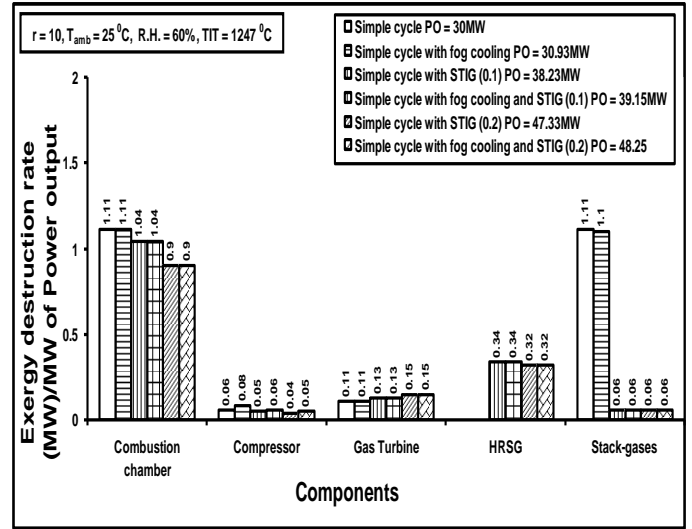
Figure 19: Exergy destruction rate (MW) per MW of output of system components for retrofitted cycles

Combustion chamber is the most sensitive component for exergy destruction because the mixing of air and high temperature STIG increases the average temperature of the air by which exergy destruction rate increases and highest for Combined cycle with STIG (0.2). It has been noted that the exergy of stack-gases has been fully utilized by STIG (0.1) cycle as the large amount of STIG increases the exergy destruction rate of stack-gases. Therefore STIG cycle can be optimized between STIG (0.1) and STIG (0.2).

Fig 19 shows the ratio of exergy destruction rate (MW) to the power output (MW) for different system components of simple and retrofitted cycles. Evaporative cooling and STIG both increases the mass flow rate of air due to which power output

Hence the exergy destruction rate (MW) per MW of power output decreases for combustion-chamber, HRSG. Evaporative cooling reduces the ratio of exergy destruction and power output for gas-turbine because the average temperature of combustion products reduces slightly and hence exergy destruction rate of gas-turbine increases gradually as compared to power output for same increment of mass flow rate. Although evaporative cooling reduces the inlet air temperature to compressor yet the increases mass flow rate enhance the exergy destruction in to the compressor.

Table 3: Comparison of performance parameters of simple and retrofitted cycles.

S.N	Performance Parameters	Simple cycle	Simple cycle+EVC	Simple cycle +STIG	Simple cycle+EVC+STIG
1.	First law efficiency (%)	30.54	30.72	72.57	72.69
2.	Second law efficiency (%)	29.51	29.70	55.3	55.2
3.	Power generation efficiency (%)	29.93	30.11	33.33	33.4
4.	Thermal efficiency (%)	30.54	30.72	34.01	34.08
5.	Heat rate (kW/kWh)	12029	11958	10800	10780
6.	Air fuel ratio	23.20	22.96	20.28	20.13
7.	Specific fuel consumption(kg/kWh)	0.2357	0.2343	0.2116	0.2112
8.	Net Power output (MW)	30	30.93	38.23	39.15
9.	Electric work done (MW)	29.4	30.31	37.46	38.36
10.	Total exergy destruction per MW of output$\sum \dot{E}_D/MW$	2.39	2.38	1.623	1.629
11.	System running cost	Very high	High	Low	Least
12.	Implementation cost	Not required	Very low	Low	Low
13.	Environmental-pollution	Very high	High	Very low	Very low

4. Conclusions

The present work analysed retrofitted gas turbine cycle energetically and exergetically. An EES program has been formulated to compute the result of analysis. A detailed

parametric analysis has been presented for the relative comparison of retrofitted cycles such as EVC, STIG and combined cycle. The comparison of various performance parameters, environmental factors and cost factors predicts and concludes that the combined effect of evaporative cooling and

STIG technology enhances the overall performance of the power generation system along with cost reducing and low environmental pollution view. As the implementation of combined technology does not require complex machine operations, construction and asset, the simple cycle gas turbines in India can be retrofitted with combined technology to obtain an energy and cost optimum system. The major concluding points are mentioned below:

- Simple cycle gas turbine has been retrofitted with a) Fog cooling (or evaporative cooling) b) STIG c) Fog cooling (or evaporative cooling) and STIG both (combined cycle), which has been included in various power generation plants in India as well as abroad. The utility of retrofitted cycles has become more significant especially in summer season whenever the density of air gets reduced by which the power output of plant falls. The power output and thermal efficiency of a simple cycle gas turbine can be triggered using combined (evaporating cooling and STIG) retrofitting technology. The NOx or SO$_2$ emission can also be reduced and controlled using above technologies which proceeds towards environment friendly power generation systems. Whenever the high temperature exhaust gases have been left in to the environment (i.e. open circuit simple cycle gas turbine, Industrial turbines for electricity production and Air-craft engines), cause thermal pollution and reduce oxygen capacity of air. As the energy of exhaust gases have been utilized at their full extent, the retrofitted technologies reduce running cost of the power generation system and leads towards a cost effective and environment-friendly system. Results of parametric study of retrofitting system have been registered at designed conditions.
- Evaporative cooling enhances the power output 3.1% and thermal efficiency 0.18% while decreases heat rate by 0.6% which proves that the EVC cycle is more efficient than that of simple cycle. However some additional maintenance cost is required to implement evaporative cooling system. The EVC has been registered its superiority over simple cycle especially for high ambient temperature and low R.H. the percentage increase in power output reaches up to 10%.
- STIG cycle improves the net power output by 27.4% and thermal efficiency by 3.5% while reduces heat rate by 10.2%. In this way the importance of STIG cycle is more than that of EVC cycle. The improvement in power output is about 9 times and in thermal efficiency is about 20 times than that of EVC cycle. Therefore the STIG cycle registers more significant results than that of EVC cycle as well as it is more environment-friendly, however some implementing cost (initial cost) is higher. The utility of STIG cycle is more significant in summer seasons (when ambient temperature and R.H. is high), the increment in power output reaches up to 36% which makes the STIG cycle superior than that of other cycles.
- Combined cycles improves the net power output by 30.5% and thermal efficiency by 3.54% while reduces heat rate by 10.4%. Therefore the combined cycle registers highest superiority among all cycles. The combined cycle is more environment friendly and cost effective however the implementing cost is little higher. The increment in power output has been registered up to 45 % during summer season at high ambient temperature (50 ^{0}C) and high R.H. (80%). The thermal efficiency also enhances up to 4.5% and second law efficiency about 26%. Therefore, the implementation of combined technology is a justified decision to obtain a energy and cost efficient power generation plant.

In the light of above points, it is observed that the retrofitted techniques improve the performance of the simple gas turbine cycle which have been incorporated with it. The retrofitted techniques are economical, simple and eco-friendly which may fulfill the peak load demand of electricity as well as save fuel consumption.

References

[1] Bhargava, R. and Meher-Homji, C. B., "Parametric analysis of existing gas turbines with inlet evaporative and overspray fogging", Journal of engineering for gas turbines and power, vol.127 issue 145 2005, pp.145-154.

[2] Chaker, M. Meher-Homji, C.B. Mee, I.I.I.T., "Inlet fogging of gas turbine engines-PartII: fog droplet sizing analysis, nozzle types, measurement, and testing", Journal of engineering for gas turbines and power vol.126 2004, pp. 559-571.

[3] Sinha, R. Bansode, S., "A thermodynamic analysis for gas turbine power optimization by fog cooling system" 20th national and 9th International ISHMT-ASME heat and mass transfer conference 2010.

[4] Moran, M.J., "Thermal System design and optimization 1996, pp. 156-158, 187-193, 517-21.

[5] Wang, F.J. Chiou, J.S. Wu, P.C., "Economic feasibility of waste heat to power conversion", Applied Energy, vol.84 2007, pp. 442-454.

[6] Kumar, A Kachhwaha, S.S. Mishra, R.S., "Thermodynamics analysis of a regenerative gas turbine cogeneration plant", Journal of Scientific & Industrial Research, vol. 69 2010, pp. 225-231.

[7] Pelster, S. Favrat, D. Von Spakovsky, M.R., "The thermo economic analysis and enivironomic modelling and optimization of the synthesis and operation of combined cycle with advanced options", Engineering for gas turbine and Power, Transaction of the ASME, vol. 123 2001, pp. 717-26.

[8] Korakianitis, T. Grantstrom, J.P. Wassingbo, P., "Parametric Performance of Combined-Cogeneration Power Plants with Various Power and Efficiency Enhancements", Engineering for gas turbine and Power, Transaction of the ASME, vol. 128 2005, pp. 65-72.

[9] Al-Hawaj, O.M. AL-Mutairi, H., "A combined power cycle with absorption air cooling", Energy, vol. 32 2007, pp. 971-982.

[10] Facchini, B. Daniele, F. Giampoalo, M., "Exergy analysis of combined cycles using latest generation gas turbines", Engineering for gas turbine and Power, Transaction of the ASME, vol. 122 2000, pp. 233-37.

[11] Nishida, K. Takagi, T. Kinoshita, S., "Regenerative stem-injection gas-turbine systems", Applied Energy, vol. 81 2005, pp. 231-246.

[12] Yadav J.P., "Exergy analysis of novel gas/steam combined cycle gas turbines configuration", ETME journal-MC, 2005.

[13] Bellorio M.B. Primenta J.M.D., "Theoretical analysis of air conditioning by evaporative cooling influence on gas turbine cycles performance", 18 International Congress of Mechanical Engineering, 2005, Ouro Preto, MG.

[14] Kumar R. N., Krishna K. R., "second law analysis of gas turbine power plant with alternative regeneration", ISHMT.Heat and mass transfer conference, 2006 Pp1813-18.

[15] Arora, A., "Energy and exergy analyses of compression, absorption, and combined cycle cooling systems", PhD thesis, Centre for Energy Studies: IIT Delhi 2009.

[16] Klein, S. A., Alvarado, F.: Engineering Equation Solver, F Chart Software, Middleton, WI. Version 9. 224-3D, 2012.

[17] Kalla, S. K., Arora, B. B., Usmani, J. A., "Alternative refrigerants for HCFC- A review", J. Thermal Engg., vol. 4 issue 3 2018, pp. 1998-2017.

[18] Srinivas T., Gupta A.V.S.S.K.S., Reddy B.V., "Sensitivity analysis of STIG based combined cycle with dual pressure HRSG", International Journal of Thermal Science, 2007, India.

[19] Bouam A., Aissani S., Kadi R., "Combustion chamber steam injection for gas turbine performance improvement during high ambient temperature operation", Journal of engineering for gas turbines and power, vol. 130 issue 0417 2008, pp. 1-10.

[20] Agarwal, S., Kachhwaha, S. S., Mishra, R. S., "Performance improvement of a simple gas turbine cycle through integration of inlet air evaporative cooling and steam injection", J. Sci. & Ind. Research, vol. 70 July 2011, pp. 544-553.

[21] Arora, B. B., Rai, J. N., "Optimization of thermal efficiency of combined cycle power generation", National seminar on energy & environment, Dec. 2001, Anand Engineering College, Agra.

Nomenclature

Abbreviations

AP	Approach point (^{0}C)
Cond.	Condenser
dbt	Dry bulb temperature (^{0}C)
$\dot{E}$	Exergy rate (kW)
$\dot{E}_D$	Exergy destruction rate (kW)
EVC	Evaporative cooling of inlet air
HRSG	Heat recovery steam generator
HR	Heat rate
$\dot{m}$	Mass flow rate
PP	Pinch point (^{0}C)
STIG	Steam injection to gas turbine
TIT	Turbine inlet temperature
U	Internal energy
wbt	Wet bulb temperature (^{0}C)